Analysis of Magnetic Microbead Capture With and Without Bacteria in a Microfluidic Device Under Different Flow Scenarios

Samuel A. Miller
Department of Mechanical and Materials Engineering,
University of Cincinnati,
598 Rhodes Hall,
Cincinnati, OH 45221
e-mail: mille4sa@mail.uc.edu

William R. Heineman
Department of Chemistry,
University of Cincinnati,
120 Crosley Tower,
P.O. Box 210172,
Cincinnati, OH 45221
e-mail: william.heineman@uc.edu

Alison A. Weiss
Department of Molecular Genetics, Biochemistry & Microbiology,
University of Cincinnati,
2254 Medical Sciences Building,
231 Albert Sabin Way,
Cincinnati, OH 45267
e-mail: alison.weiss@uc.edu

Rupak K. Banerjee[1]
Fellow ASME
Department of Mechanical and Materials Engineering,
University of Cincinnati,
593 Rhodes Hall, ML 0072,
Cincinnati, OH 45221
e-mail: rupak.banerjee@uc.edu

Efficient detection of pathogens is essential for the development of a reliable point-of-care diagnostic device. Magnetophoretic separation, a technique used in microfluidic platforms, utilizes magnetic microbeads (mMBs) coated with specific antigens to bind and remove targeted biomolecules using an external magnetic field. In order to assure reliability and accuracy in the device, the efficient capture of these mMBs is extremely important. The aim of this study was to analyze the effect of an electroosmotic flow (EOF) switching device on the capture efficiency (CE) of mMBs in a microfluidic device and demonstrate viability of bacteria capture. This analysis was performed at microbead concentrations of 2×10^6 beads/mL and 4×10^6 beads/mL, EOF voltages of 650 V and 750 V, and under constant flow and switching flow protocols. Images were taken using an inverted fluorescent microscope and the pixel count was analyzed to determine to fluorescent intensity. A capture zone was used to distinguish which beads were captured versus uncaptured. Under the steady-state flow protocol, CE was determined to range from 31% to 42%, while the switching flow protocol exhibited a CE of 71–85%. The relative percentage increase due to the utilization of the switching protocol was determined to be around two times the CE, with $p < 0.05$ for all cases. Initial testing using bacteria-bead complexes was also performed in which these complexes were captured under the constant flow protocol to create a calibration curve based on fluorescent pixel count. The calibration curve was linear on a log-log plot, with R^2-value of 0.96. The significant increase in CE highlights the effectiveness of flow switching for magnetophoretic separation in microfluidic devices and prove its viability in bacterial analysis.
[DOI: 10.1115/1.4040563]

Keywords: magnetophoretic separation, magnetic microbeads, capture efficiency, electroosmotic flow, switching

1 Introduction

Micro total analysis devices, often referred to as lab-on-chip devices, are a burgeoning field that have led to the development of new technologies required to perform biological assay in a small, portable device [1]. These devices are designed to handle micro- to nano-liter samples and produce reliable and rapid results for on-site diagnostics and screening. The challenge with applying these devices to biological assay is the implementation of laboratory scale processes, such as cell culture, biochemical testing, immunoassay, and microscopy that require multiple and larger size equipment or wait times into a portable device [2].

Magnetophoretic separation based immunoassay is a popular technique that uses magnetic microbeads (mMBs) coated with antibodies for specific cell surface epitopes in order to tag and isolate particular biomolecules [3–6]. Separation is achieved by applying a magnetic field to the device to induce magnetophoretic mobility and isolate the biomolecules attached to mMBs. The mMBs have a large surface area-to-volume ratio, can be functionalized with a variety of antibodies, and are easily manipulated via magnetic field without undue disturbance to the attached biomolecules [7–9]. The targeting versatility as well as the reliable and efficient separation processes makes magnetophoretic immunoassay an ideal candidate for implementation into micro total analysis devices.

Kwon et al. used streptavidin-coated mMBs combined with fluorescent antibodies to detect toxins [6]. Thompson et al. studied how the use of microwells would affect the capture of mMBs [10]. This study reported a low capture efficiency (CE) (around 13%). Beyor et al. designed special pumps that showed how pulsatile flow improved the capture of mMBs by driving the solution back and forth through multiple passes, showing improved capture efficiencies up to 70 [5]. Ramadan et al. examined how electromagnets perform in a device to better control and isolate mMBs but used a silicon wafer instead of transparent glass as the slide and used a high pressure syringe pump to drive the flow [11]. Munir et al. studied how different magnet positions around a circular chamber affect the trapping efficiency of mMBs in a channel [12]. This study performed only a numerical analysis while also modeling a parabolic fluid profile characteristic of pressure-driven flow. A study by Di Carlo et al. uses a process called inertial focusing to organize mMBs based on the streamlines in a microchannel [13]. This requires a series of s-shaped bends in an effort to create an ordered line of mMBs at the outlet. Channel geometry was analyzed by Zhang et al. as part of a numerical experiment in an effort to create a filtering mechanism based on particle size [14]. A study by Li et al. evaluated introducing obstacles to a microchannel to adjust the flow streamlines [15]. A study by Hoshino et al. explored alternating magnet polarities along a channel to isolate mMBs and cancer cells from blood [16]. However, these studies utilize pressure-driven flow instead of electroosmotic flow (EOF), resulting in different flow profiles in the channel. To the best of the authors knowledge, none of these publications reported mMB capture using electroosmotic flow, instead opting for pressure-driven pumps to drive the flow. These are often prone

[1]Corresponding author.
Manuscript received February 13, 2018; final manuscript received May 4, 2018; published online September 21, 2018. Assoc. Editor: Yaling Liu.

to leakage during field testing, complicated, and expensive. In addition, the higher pressure necessary to pump the fluid through the small microchannels also causes seepage at the edges of the bonds between the polymer and the slide.

1.1 Previous Study. Efficient capture of mMBs is important for the sensitivity and effectiveness of any proposed microfluidic lab-on-chip device. EOF has an advantage over mechanically driven pumps due to it being inexpensive and efficient to build for operating at small volumes [17,18]. The use of EOF allows greater control over the magnitude and direction of the flow [19]. A previous study in our group, by Das et al., analyzes a device utilizing an EOF-driven switching mechanism and permanent Neodymium (NdFeB) magnet perpendicular to the channel to improve mMB immobilization [20]. The Das et al. study characterized the capture of mMBs due to fluorescent intensity of captured mMBs at different mMB concentrations and flow rates in comparison to a standard fluorescence of known concentration samples. *However, the Das* et al. *study has a limitation due to the inability of the analysis method to accurately determine the number of mMBs that are run through the device but escape capture*. Without accounting for the escaped mMBs, the assessment of capture efficiency remains limited, preventing the determination of the accuracy and reliability of the device.

1.2 Proposed Design. This study provides improved analysis of the capture efficiency of the device designed previously by our group and published in Das et al. [20]. It is important to efficiently capture the mMBs in order to produce accurate and reliable results with the greatest sensitivity possible. Therefore, the determination of the capture efficiency, i.e., the ratio of the number of mMBs captured to the number of mMBs injected into the channel, would determine whether any device is dependable.

The previous studies have shown how multiple passes can increase capture of mMBs using the implementation of a switching protocol to return initially uncaptured mMBs to the device [5,20]. It was *hypothesized* that the switching protocol integrated into this device will return the mMBs to the area of higher magnetic field, allowing for more mMBs to be captured, and thus increasing the capture efficiency. To address the limitations of the Das et al. study, *this research implements a unique capture zone to identify the area where mMBs can be captured, thereby isolating mMBs that are run through the device but left uncaptured*. Therefore, it is possible to accurately determine a true capture efficiency by comparing the fluorescent intensity of the captured and uncaptured mMBs at multiple mMB concentrations and EOF voltages. The device also underwent initial testing using *fluorescent bacteria-mMB complexes, and a calibration curve was created* using the constant flow protocol. This verifies the device's ability to capture bacteria complexes and differentiate between concentrations based on fluorescent intensity.

2 Methods

This section describes the methods used to create the device, the materials used, the design of the experiment, and the analysis performed. Fluorescent tagged mMBs were driven through the channel using EOF, immobilized using an external magnet, and characterized using inverted fluorescent microscopy. The images were analyzed to determine the total fluorescence of captured and uncaptured mMBs, allowing for the calculation of capture efficiency.

2.1 System Properties. The microfluidic device was created through standard soft lithography technique with polydimethylsiloxane (PDMS) according to the procedure presented in Das et al. [20]. The resulting device consists of PDMS bonded to a glass slide to create a 50 mm channel with a cross section of 50 μm $\times$ 50 μm with 6 mm diameter wells at each end of the channel.

The mMBs used in the experiments were 2.8 μm diameter Dynabead M280 Sheep anti-Rabbit IgG mMBs tagged with an Alexa Fluor 488 Rabbit anti-Mouse IgG fluorescent marker, as shown in Fig. 1(*a*), following the procedure in Das et al. [20]. The microbeads were run through the system at concentrations of 2×10^6 and 4×10^6 beads/mL. The magnet used in the experiments was a 1/8 in $\times$ 1/8 in $\times$ 3/8 in volume neodymium (NdFeB) magnet.

For the bacterial tests, the same mMBs were used in conjunction with a Virostat Rabbit polyclonal anti-*E. coli* binding antibody to bind to fluorescent *E. coli*, as shown in Fig. 1(*b*). This created a bacteria-mMB complex that would allow the bacteria to be captured through magnetic separation, but prevent unpaired mMBs from producing incorrect results since only the bacteria is fluorescent. This also allowed the use of excess microbeads to

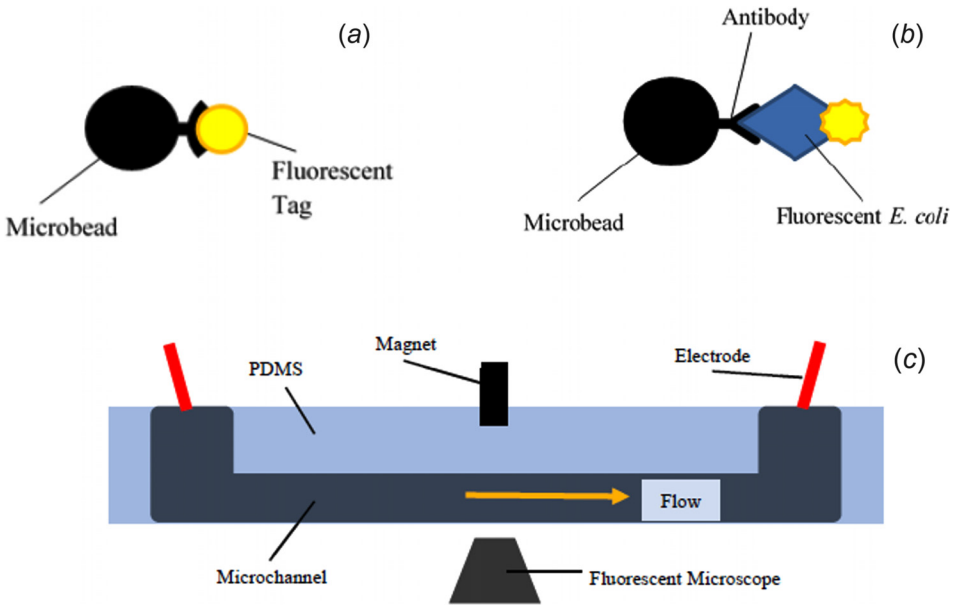

Fig. 1 Schematics (not to scale) of (*a*) fluorescently tagged beads, (*b*) mMB-fluorescent bacteria complexes, and (*c*) device setup used in experiments

ensure maximum bacteria capture without increasing the potential for inflated fluorescent results.

2.2 Experimental Method. The experimental preparation procedure outlined in Das et al. was followed for this study [20]. The channel was treated with 1M NaOH solution for 10 min, washed with PBS buffer and, prior to each experiment, primed with a 1% Tween 20 in PBS buffer solution for 5 min to decrease the surface tension and prevent the mMBs from sticking to the channel walls while not captured.

The mMB solution was injected into the inlet well and the chip was placed on an inverted fluorescent microscope using a xenon arc lamp with a filter for the Alexa Fluor 488 (excitation wavelength: 495 nm, emission wavelength: 519 nm). The magnet was

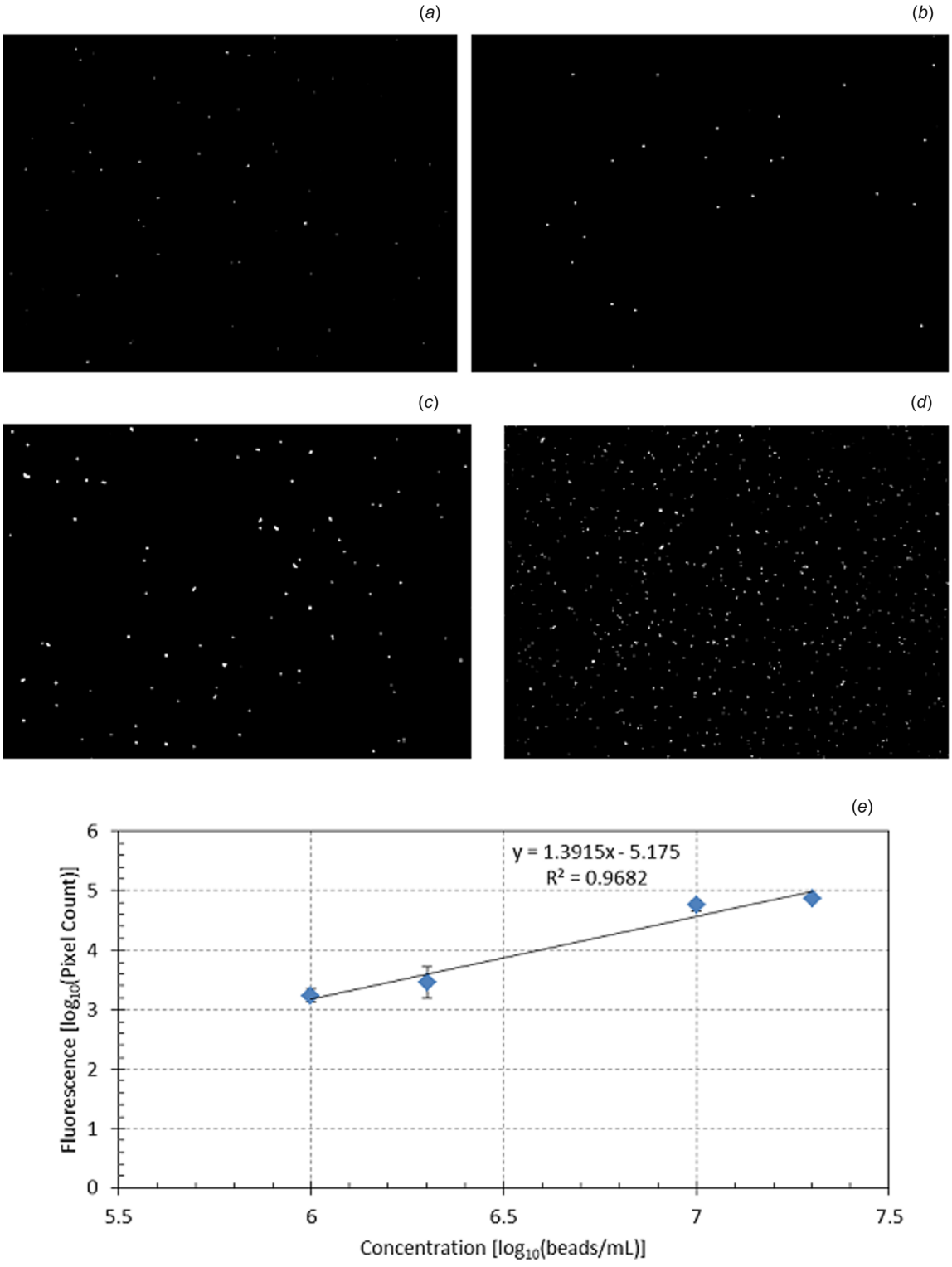

Fig. 2 Image of fluorescence from sample with concentration of (*a*) 1×10^6 beads/mL, (*b*) 2×10^6 beads/mL, (*c*) 1×10^7 beads/mL, (*d*) 2×10^7 beads/mL, and (*e*) calibration curve of fluorescence as a function of mMB concentration

put in place and two platinum electrodes were connected to a high voltage sequencer to drive the flow at voltages of 650 V and 750 V for 20 min, with the flow switching voltage profiles discussed in the *Results*. A diagram of the experimental setup is shown in Fig. 1(*c*).

In order to better analyze the device, a capture zone calibration test was performed to determine the maximum capture zone for analysis. This test was performed by passing mMBs through the channel at the lowest flow rate and then immediately running buffer to clear uncaptured mMBs. The channel was then analyzed to determine the distance before and after the magnet where mMBs were captured. During experiments, mMBs before the capture zone are not considered since they did not enter the test, mMBs in the capture zone were determined to be captured, and mMBs after the capture zone and in the outlet well were determined to be missed.

2.3 Characterization. The gathered images were analyzed in MATLAB to determine the fluorescent intensity based on pixel count. The determination of capture zone allows for a unique characterization method that allows the calculation of a capture efficiency based on the ratio of the number of mMBs captured to the number of total mMBs run in the experiment. Statistical analysis was then performed using a t-test, with a resulting $p < 0.05$ proving statistically significant.

The initial bacteria results were analyzed using the same process of image collection and processing. However, the raw fluorescent pixel counts were used to create a fluorescent calibration curve based on total fluorescence and bacteria concentration. The calibration curve was created at varying concentrations under the constant flow protocol at 650 V, with $n = 3$ for each concentration.

3 Results

Capture percentage was determined for mMB concentrations of 2×10^6 and 4×10^6 beads/mL, EOF voltages of 650 and 750 V, and under constant flow and switching flow protocols. Fluorescent images were taken of samples with known concentrations to determine a calibration curve based on fluorescent intensity.

3.1 Fluorescence Calibration of Magnetic Microbeads. Samples of known concentration of fluorescently tagged mMBs were put on a microscope slide and imaged using fluorescent microscopy, with images for various concentrations shown in Figs. 2(*a*)–2(*d*). These images were analyzed to determine the fluorescent intensity in terms of pixel count associated with each known concentration. These results are shown as a function of concentration in Fig. 2(*e*) in the form of a calibration curve. This curve can be used to determine effective concentration of beads captured given unknown inlet samples.

3.2 Constant Flow and Switching Flow. Constant and flow switching protocols were compared in an effort to assess the increase in the capture efficiency of mMBs in the device. The constant flow protocol uses a fixed potential difference along the channel to drive a constant flow from inlet to outlet over the entire 20 min test period with the flow rate calculated according to the Helmholtz–Smoluchowski Equation, as shown in the following equation:

$$U_{ep} = -\frac{E_z \varepsilon_r \varepsilon_o \zeta_p}{\mu} \tag{1}$$

where U_{ep} is the velocity (cm/s), E_z is the applied electric field (V/cm), ε_r is the dielectric constant of the medium, ε_o is the vacuum permittivity (F/m), ζ_p is the zeta potential (V), and μ is the dynamic viscosity (Pa·s). For the 650 V case, E_z is 130 V/cm, ε_r is 80.4, ε_o is 8.55×10^{-12} F/m, ζ_p is −95.6 mV, and μ is 8.6×10^{-4} Pa·s [20,21]. The fluid velocity at this voltage was determined to be 0.099 cm/s, which equates to a volumetric flow rate of 0.15 μL/min. The switching protocol aims to increase capture by alternating flow direction by changing the voltage at the inlet and outlet to increase mMB residence time in the capture zone. The switching protocol runs for 8 min forward followed by two periods of alternating 3 min backward then 3 min forward, for a 20 min total testing time. With a 5 cm long channel and EOF flow rates of 0.099 cm/s and 0.115 cm/s for the 650 and 750 V cases, respectively, a 3 min run time would allow for about 3.5 and 4 full channel length (5 cm) clearances at the two voltages. This allowance for multiple full flows through the channel helps ensure that a high quantity of mMBs is available to be analyzed.

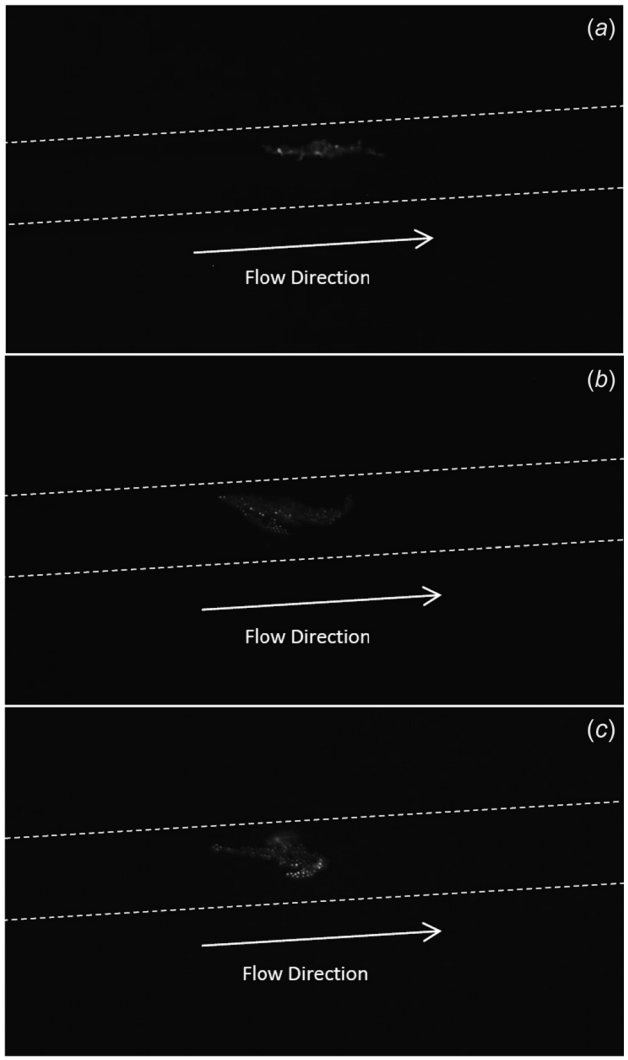

Fig. 3 Captured mMBs from (*a*) 2×10^6 beads/mL sample at 750 volts using constant protocol, (*b*) 4×10^6 beads/mL sample at 650 volts using switching protocol, and (*c*) 4×10^6 beads/mL sample at 750 volts using switching protocol

3.3 Capture Efficiency of Constant Flow and Switching Flow Protocols. Fluorescent tagged mMBs in solutions of 2×10^6 and 4×10^6 beads/mL were run through the device using both switching and constant flow protocols at voltages of 650 and 750 V, with images taken along the channel. Sample images of captured mMBs at 2×10^6 beads/mL, 750 V, and constant flow; 4×10^6 beads/mL, 650 V, and switching flow; and 4×10^6 beads/mL, 750 V and switching flow are shown in Figs. 3(*a*)–3(*c*), respectively. The images were then analyzed, with mMBs imaged within the capture zone counted as captured and mMBs located

after the capture zone counted as uncaptured. Those mMBs located before the capture zone were not considered since they did not ever enter the test scenario.

The *capture efficiency* (η_c) of the device was determined using Eq. (2), with the *relative percent difference* between the constant and switching flow protocols calculated using Eq. (3)

$$\eta_c = \frac{\text{pixel count captured}}{\text{pixel count captured} + \text{pixel count uncaptured}} \tag{2}$$

$$\text{relative \% difference} = \frac{\eta_{c\_switch} - \eta_{c\_constant}}{\eta_{c\_constant}} \tag{3}$$

The relative percent difference between the switching and constant flow obtained from this experiment was compared to the results of the Das et al. experiment, as shown in Fig. 4 [20]. The present experiment shows a much higher η_c, with a relative percent difference increase of 99% and 122% compared to 9% and 52% between switching flow and constant flow for the 650 V and 750 V, respectively [20]. This improvement is due to the analysis of beads that are run through the system but remained uncaptured. In the Das et al. experiment, η_c is calculated where only the captured beads were accounted for [20]. Moreover, the total number of mMBs passing through the device is higher for the constant flow than the switching flow, causing an increased constant flow fluorescence. This resulted in a smaller difference between the two protocols. Since the present experiment accounts for the number of uncaptured beads that are run through the system, an accurate comparison can be made between the switching and constant flows.

The parameter η_c for the 650 V and 750 V scenarios is shown in Figs. 5(*a*) and 5(*b*), respectively. For all concentrations and voltages, η_c of mMBs was significantly higher for the switching flow protocol (71–85%) versus the constant flow protocol (31–42%), with a *relative percentage difference* of around two times η_c with $p < 0.05$ for all cases. This significant increase in η_c shows the effectiveness of the flow switching in returning the initially uncaptured mMBs to the capture zone, while those mMBs remain uncaptured in the constant flow case.

3.4 Bacteria Calibration Curve Under Constant Flow Protocol. Initial bacteria testing provided a calibration curve of fluorescent intensity as a function of concentration under the constant flow protocol at 650 V. This curve is linear on a log-log plot with a R^2 value of 0.96, as shown in Fig. 6. There is an increase in total fluorescent pixel count as bacteria concentration in the sample increases, with $p < 0.05$ for each comparison of fluorescent intensity between neighboring concentrations.

4 Discussion

This study expands on the Das et al. results previously published by our group through the measure of an improved capture efficiency. While the total fluorescence measured in the Das et al. study can help determine the sensitivity of the device and fluorescent difference at various concentrations, it has a shortcoming in that it cannot accurately compare η_c of mMBs for different scenarios [20]. This study uses a unique approach to determine the improved η_c of the device by comparing the number of mMBs that are captured to the total number of mMBs run through the device.

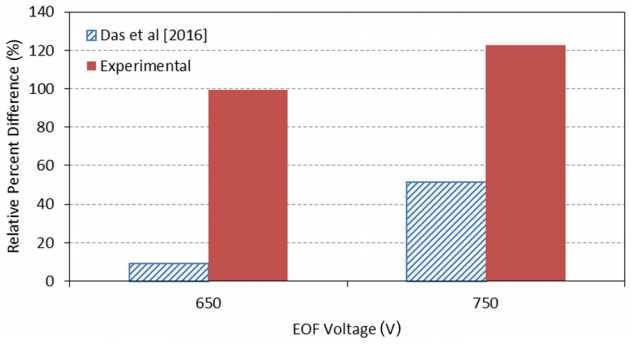

Fig. 4 Comparison of relative percent difference between switching and constant flow protocols for 2×10^6 beads/mL samples for this experiment and Das et al. [20]

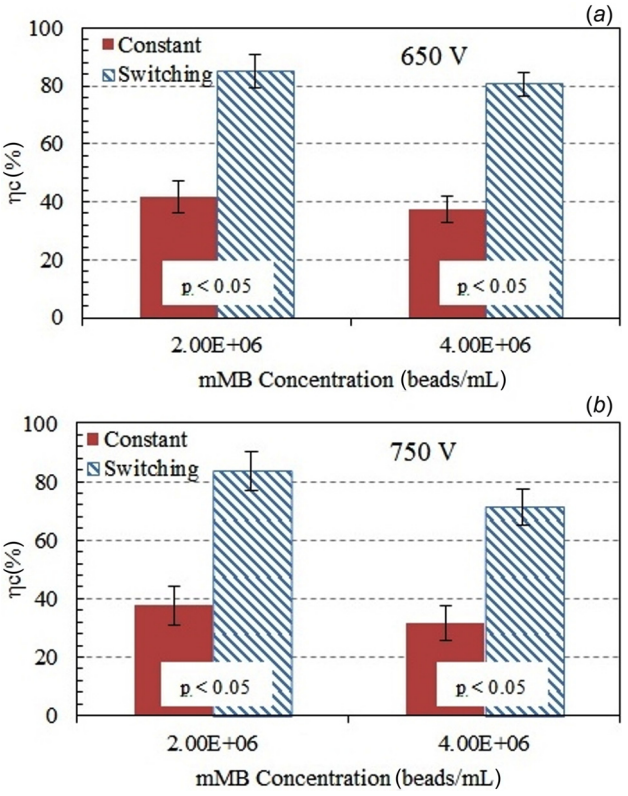

Fig. 5 Capture efficiency of mMBs under switching and constant protocols at (*a*) 650 V and (*b*) 750 V

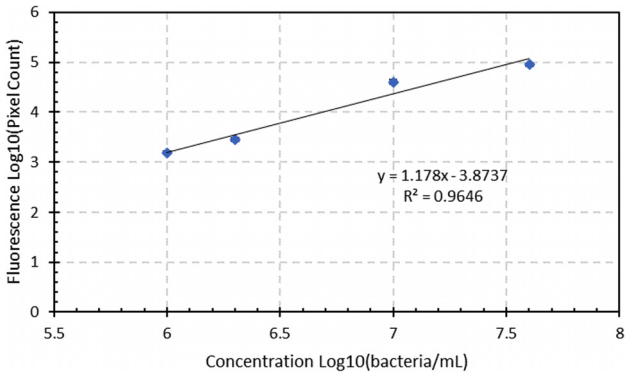

Fig. 6 Calibration curve of bacteria-mMB complex under constant flow protocol at 650 V

4.1 Capture Zone. The determination of the capture zone is an important aspect for determining η_c in this study. Bead capture is determined by the balance between the horizontal momentum and drag forces and vertical magnetic forces acting on the mMBs. When the net horizontal force is much greater than the magnetic force, the mMB escapes while the mMB is captured if the magnetic force is much greater than the net horizontal force. Since the magnetic force is constant for all situations, the maximum bead capture will occur at the lowest fluid velocity. Therefore, the

minimum EOF voltage of 650 V is used in the determination of capture zone since it produces the lowest fluid velocity.

4.2 Capture Efficiency Under Constant and Switching Flows. The parameter η_c associated with the switching protocol was about two times larger than the η_c under the constant flow protocol for all conditions. Under constant flow, the mMBs only make one pass by the magnet, so any mMB that avoids initial capture is lost. However, under the flow switching protocol, mMBs that are not initially captured have a chance to return to the area of higher magnetic force due to the switching of the horizontal forces and, therefore, have an increased opportunity to be captured. This increased residence time in the capture zone produces significantly higher capture efficiencies associated with the switching protocol. The increase of η_c from approximately 42% under constant flow to around 85% under switching flow is critical in minimizing the error in the future application of isolating pathogens using the device.

4.3 Bacteria Calibration Curve Under Constant Flow. The initial log-log calibration curve shows a linear comparison, highlighting the consistency of bacteria capture within the device. Additionally, the statistically significant p-values when comparing neighboring concentrations demonstrate the feasibility of the device to accurately and reliably differentiate between concentrations in unknown samples.

4.4 Limitations of Experiment. The exact number of mMBs captured could not be counted; therefore, quantification using fluorescent images was used. The parameter η_c was only analyzed for a stationary magnet instead of electromagnets, which are popular in microfluidic devices.

4.5 Future Direction. Further bacteria experiments will be performed to analyze this device by immobilizing a mMB-pathogen-fluorescent tag complex in the channel under switching flow. This will involve determining capture efficiency of these bacteria-mMB complexes and then create a calibration curve for fluorescence under switching flow. This could make it possible to better use the device to accurately determine concentration of bacteria in unknown samples. In addition, some parameters, such as switching frequency, EOF voltage, and channel geometry, need to be optimized for improved performance.

Acknowledgment

This research study was supported by the National Institute for Occupational Safety and Health through the University of Cincinnati Education and Research Center Grant No. T42OH008432.

Funding Data

- National Institute for Occupational Safety and Health (T42OH008432).

Nomenclature

EOF = electroosmotic flow
E_z = applied electric field (V/cm)
mMB = magnetic microbead
NdFeB = neodymium alloy
PDMS = polydimethylsiloxane
U_{ep} = EOF velocity (cm/s)
ε_o = vacuum permittivity (F/m)
ε_r = relative permittivity of the fluid
η_c = capture efficiency (%)
ς_p = zeta potential (V)

References

[1] Manz, A., Graber, N., and Widmer, H. Á., 1990, "Miniaturized Total Chemical Analysis Systems: A Novel Concept for Chemical Sensing," Sens. Actuators B: Chem., **1**(1–6), pp. 244–248.
[2] Deisingh, A. K., and Thompson, M., 2004, "Biosensors for the Detection of Bacteria," Can. J. Microbiol., **50**(2), pp. 69–77.
[3] McCloskey, K. E., Chalmers, J. J., and Zborowski, M., 2003, "Magnetic Cell Separation: Characterization of Magnetophoretic Mobility," Anal. Chem., **75**(24), pp. 6868–6874.
[4] Choi, J.-W., 2006, "Fabrication of Micromachined Magnetic Particle Separators for Bioseparation in Microfluidic Systems," *Microfluidic Techniques* (Methods In Molecular Biology™), Humana Press, New York, pp. 65–81.
[5] Beyor, N., Seo, T. S., Liu, P., and Mathies, R. A., 2008, "Immunomagnetic Bead-Based Cell Concentration Microdevice for Dilute Pathogen Detection," Biomed. Microdevices, **10**(6), pp. 909–917.
[6] Kwon, Y., Hara, C. A., Knize, M. G., Hwang, M. H., Venkateswaran, K. S., Wheeler, E. K., Bell, P. M., Renzi, R. F., Fruetel, J. A., and Bailey, C. G., 2008, "Magnetic Bead Based Immunoassay for Autonomous Detection of Toxins," Anal. Chem., **80**(22), pp. 8416–8423.
[7] Choi, J.-W., Liakopoulos, T. M., and Ahn, C. H., 2001, "An On-Chip Magnetic Bead Separator Using Spiral Electromagnets With Semi-Encapsulated Permalloy," Biosens. Bioelectron., **16**(6), pp. 409–416.
[8] Gijs, M. A., 2004, "Magnetic Bead Handling On-Chip: New Opportunities for Analytical Applications," Microfluid. Nanofluid., **1**(1), pp. 22–40.
[9] Guo, S., Deng, Y., Zhao, L., Chan, H., and Zhao, X., 2008, "Effect of Patterned Micro-Magnets on Superparamagnetic Beads in Microchannels," J. Phys. D: Appl. Phys., **41**(10), p. 105008.
[10] Thompson, J. A., Du, X., Grogan, J. M., Schrlau, M. G., and Bau, H. H., 2010, "Polymeric Microbead Arrays for Microfluidic Applications," J. Micromech. Microeng., **20**(11), p. 115017.
[11] Ramadan, Q., Poenar, D. P., and Yu, C., 2009, "Customized Trapping of Magnetic Particles," Microfluid. Nanofluid., **6**(1), pp. 53–62.
[12] Munir, A., Wang, J., and Zhou, H., 2009, "Dynamics of Capturing Process of Multiple Magnetic Nanoparticles in a Flow Through Microfluidic Bioseparation System," IET Nanobiotechnol., **3**(3), pp. 55–64.
[13] Di Carlo, D., Irimia, D., Tompkins, R. G., and Toner, M., 2007, "Continuous Inertial Focusing, Ordering, and Separation of Particles in Microchannels," Proc. Natl. Acad. Sci., **104**(48), pp. 18892–18897.
[14] Zhang, Z., Xu, J., Hong, B., and Chen, X., 2014, "The Effects of 3D Channel Geometry on CTC Passing Pressure–Towards Deformability-Based Cancer Cell Separation," Lab a Chip, **14**(14), pp. 2576–2584.
[15] Li, P., Stratton, Z. S., Dao, M., Ritz, J., and Huang, T. J., 2013, "Probing Circulating Tumor Cells in Microfluidics," Lab a Chip, **13**(4), pp. 602–609.
[16] Hoshino, K., Huang, Y.-Y., Lane, N., Huebschman, M., Uhr, J. W., Frenkel, E. P., and Zhang, X., 2011, "Microchip-Based Immunomagnetic Detection of Circulating Tumor Cells," Lab a Chip, **11**(20), pp. 3449–3457.
[17] Comandur, K. A., Bhagat, A. A. S., Dasgupta, S., Papautsky, I., and Banerjee, R. K., 2010, "Transport and Reaction of Nanoliter Samples in a Microfluidic Reactor Using Electro-Osmotic Flow," J. Micromech. Microeng., **20**(3), p. 035017.
[18] Al-Rjoub, M. F., Roy, A. K., Ganguli, S., and Banerjee, R. K., 2012, "Enhanced Electro-Osmotic Flow Pump for Micro-Scale Heat Exchangers," ASME Paper No. MNHMT2012-75026.
[19] Husain, A., and Kim, K.-Y., 2011, "Thermal Transport and Performance Analysis of Pressure-and Electroosmotically-Driven Liquid Flow Microchannel Heat Sink With Wavy Wall," Heat Mass Transfer, **47**(1), pp. 93–105.
[20] Das, D., Al-Rjoub, M. F., Heineman, W. R., and Banerjee, R. K., 2016, "Efficient Capture of Magnetic Microbeads by Sequentially Switched Electroosmotic Flow—An Experimental Study," J. Micromech. Microeng., **26**(5), p. 055013.
[21] Dasgupta, S., Bhagat, A. A. S., Horner, M., Papautsky, I., and Banerjee, R. K., 2008, "Effects of Applied Electric Field and Microchannel Wetted Perimeter on Electroosmotic Velocity," Microfluid. Nanofluid., **5**(2), pp. 185–192.